

Automatic Registration and Error Color Maps to Improve Accuracy for Navigated Bone Tumor Surgery Using Intraoperative Cone-Beam CT

Axel Sahovaler, MD*, Michael J. Daly, PhD*, Harley H.L. Chan, PhD, Prakash Nayak, MD, Sharon Tzelnick, MD, Michelle Arkhangorodsky, BSc, Jimmy Qiu, MSc, Robert Weersink, PhD, Jonathan C. Irish, MD, MSc, FRCSC, Peter Ferguson, MD, MSc, FRCSC, and Jay S. Wunder, MD, MSc, FRCSC

Investigation performed at the University Health Network, Toronto, Ontario, Canada

Background: Computer-assisted surgery (CAS) can improve surgical precision in orthopaedic oncology. Accurate alignment of the patient's imaging coordinates with the anatomy, known as registration, is one of the most challenging aspects of CAS and can be associated with substantial error. Using intraoperative, on-the-table, cone-beam computed tomography (CBCT), we performed a pilot clinical study to validate a method for automatic intraoperative registration.

Methods: Patients who were ≥ 18 years of age, had benign bone tumors, and underwent resection were prospectively enrolled. In addition to inserting a navigation tracking tool into the exposed bone adjacent to the surgical field, 2 custom plastic ULTEM tracking tools (UTT) were attached to each patient's skin adjacent to the tumor using an adhesive. These were automatically localized within the 3-dimensional CBCT volume to be used as image landmarks for registration, and the corresponding tracker landmarks were captured using an infrared camera. The main outcomes were the fiducial registration error (FRE) and the target registration error (TRE). The navigation time was recorded.

Results: Thirteen patients with benign tumors in the femur ($n = 10$), tibia ($n = 2$), and humerus ($n = 1$) underwent navigation-assisted resections. The mean values were 0.67 ± 0.15 mm (range, 0.47 to 0.97 mm) for FRE and 0.83 ± 0.51 mm (range, 0.42 to 2.28 mm) for TRE. Registration was successful in all cases. The mean time for CBCT imaging and tracker registration was 7.5 minutes.

Conclusions: We present a novel automatic registration method for CAS exploiting intraoperative CBCT capabilities, which provided improved accuracy and reduced operative times compared with more traditional methods.

Clinical Relevance: This proof-of-principle study validated a novel process for automatic registration to improve the accuracy of resecting bone tumors using a surgical navigation system.

In orthopaedic oncology, postoperative positive margins in primary malignant bone tumors correlate directly with recurrence and patient survival^{1,2}, but negative margins can be difficult to achieve in pelvic and peri-articular locations. Current principles include oncologically safe resections while retaining sufficient uninvolved tissues to allow limb reconstruction^{3,4}.

Computer-assisted surgery (CAS) aims to improve surgical precision. This approach integrates computed tomography (CT) and magnetic resonance imaging (MRI) to plan and intraoperatively execute an operation, using navigation techniques and software⁵. CAS represents an improvement over traditional techniques such as correlating anatomic landmarks

with measurements on preoperative imaging⁶ or relying on fluoroscopy⁷. CAS showed promising results in pelvic^{8,9} and extremity¹⁰⁻¹² surgery, facilitating planning, accuracy of tumor resection, and joint preservation⁵. Furthermore, operating rooms with intraoperative 3-dimensional (3D) imaging capability present a new opportunity for CAS development and are becoming more readily available. On-the-table 3D imaging using cone-beam CT (CBCT) can be used for navigation system registration, resection assessment, and confirmation of post-resection reconstruction, thus improving surgical proficiency¹³⁻¹⁵.

Accurate alignment of the patient's imaging and anatomy, known as image-to-patient registration, is a challenging aspect of

*Axel Sahovaler, MD, and Michael J. Daly, PhD, contributed equally to this work.

Disclosure: The **Disclosure of Potential Conflicts of Interest** forms are provided with the online version of the article (<http://links.lww.com/JBJSOA/A386>).

Copyright © 2022 The Authors. Published by The Journal of Bone and Joint Surgery, Incorporated. All rights reserved. This is an open-access article distributed under the terms of the [Creative Commons Attribution-Non Commercial-No Derivatives License 4.0](https://creativecommons.org/licenses/by-nc-nd/4.0/) (CCBY-NC-ND), where it is permissible to download and share the work provided it is properly cited. The work cannot be changed in any way or used commercially without permission from the journal.

CAS^{16,17}. Different methods have been developed to address registration, as errors in this process determine the navigation accuracy and surgical outcomes. The most common registration method is a combination of fiducial-based registration and surface matching¹⁸⁻²⁰. As the fiducials typically consist of osseous anatomical points, their identification can be imprecise, and refinement by surface tracing along the exposed bone is often required. This method can be time-consuming and frustrating²¹ and can force the dissection of more healthy bone surface than needed. The availability of intraoperative 3D imaging enables registration to occur at the same time as imaging, which permits the use of alternative registration techniques employing more precise fiducials.

Using intraoperative imaging with on-the-table CBCT, we performed a pilot clinical study aiming to report, analyze, and validate a new method for automatic registration.

Materials and Methods

Study Population

Thirteen patients who were ≥ 18 years of age and had symptomatic benign bone tumors requiring surgical resection, including 12 osteochondromas and 1 osteoid osteoma, were enrolled in this study. Osteochondromas were chosen because they are excised without the need for navigation, and failure of the technology would not impact outcomes. The single patient with a symptomatic osteoid osteoma had 2 prior failed radiofrequency ablation (RFA) attempts. Our institutional research ethics board approved the study. The median patient age was 26 years (range, 20 to 47 years), and 8 patients were male. The primary tumor locations were the femur ($n = 10$ patients), the tibia ($n = 2$), and the humerus ($n = 1$) (Table I).

Image-Guided Operating Room

Surgical procedures were conducted in the Guided Therapeutics (GTx) operating room, which integrates an Artis Zeego (Siemens Healthcare) system for intraoperative CBCT imaging^{13,22} (Fig. 1).

This system is based on a flat-panel detector ($1,920 \times 2,480$) and x-ray source (up to 125 kV) mounted on a robotic C-arm gantry. CT acquisition consisted of 248 x-ray projections obtained during a 10-second orbit, yielding images encompassing $25 \times 25 \times 18$ cm using 0.5-mm^3 voxels.

The custom navigation software (GTx-Eyes) provides different 3D visualizations, including triplanar views, bone-surface renderings, and clipping planes²³. It also provides real-time feedback on the location and trajectory of planar cutting instruments in 2D and 3D views (Fig. 2). This has been validated in preclinical orthopaedic oncology studies in pelvic and extremity models^{24,25} and in head and neck surgery^{26,27}. Various cutting instruments can be navigated using an intraoperative calibration jig (see Appendix Supplemental Figure 1).

Registration of the Navigation System

Figure 3 summarizes the workflow. A rigid reference tracker was mounted to the bone adjacent to the tumor using cortical pins to track patient movement during navigation (Fig. 3-A). Two ULTEM plastic (polyetherimide; SABIC) tracking tools (UTTs), with optical spheres attached, were attached to the skin adjacent to the tumor using an adhesive (Fig. 3-A). The UTTs act as surrogates for anatomic fiducial points to provide a flexible registration mechanism and were only present during imaging (Fig. 3-B). The sphere positions were captured by the overhead infrared camera (Fig. 3-C), and the corresponding positions in the CBCT images were localized using an automatic detection algorithm (Fig. 3-D). This process eliminated the need for surgeons to manually localize anatomic points or perform surface tracing, minimizing operating room time and sources of error. The registration outcome was visualized with color-coded error maps, as described below (Fig. 3-E). Surgical resection was navigation-assisted (Fig. 3-F).

Two registration errors were reported by the navigation system: (1) the fiducial registration error (FRE), which is a

TABLE I Summary of Study Participants

| Patient No. | Sex | Age (yr) | Site | Location | Diagnosis |
|-------------|--------|----------|---------|-----------------------------|-----------------|
| 1 | Male | 25 | Femur | Right distal medial | Osteochondroma |
| 2 | Male | 26 | Femur | Left distal lateral | Osteochondroma |
| 3 | Male | 32 | Femur | Right distal | Osteochondroma |
| 4 | Female | 34 | Tibia | Right posterior lateral | Osteochondroma |
| 5 | Male | 21 | Femur | Left distal lateral | Osteochondroma |
| 6 | Female | 28 | Femur | Left distal lateral | Osteochondroma |
| 7 | Male | 23 | Femur | Right distal lateral | Osteochondroma |
| 8 | Female | 22 | Tibia | Left anteromedial | Osteochondroma |
| 9 | Male | 21 | Femur | Right distal posterolateral | Osteoid Osteoma |
| 10 | Female | 21 | Femur | Right distal medial | Osteochondroma |
| 11 | Male | 21 | Femur | Right distal | Osteochondroma |
| 12 | Female | 47 | Femur | Left proximal anterior | Osteochondroma |
| 13 | Male | 20 | Humerus | Left proximal lateral | Osteochondroma |

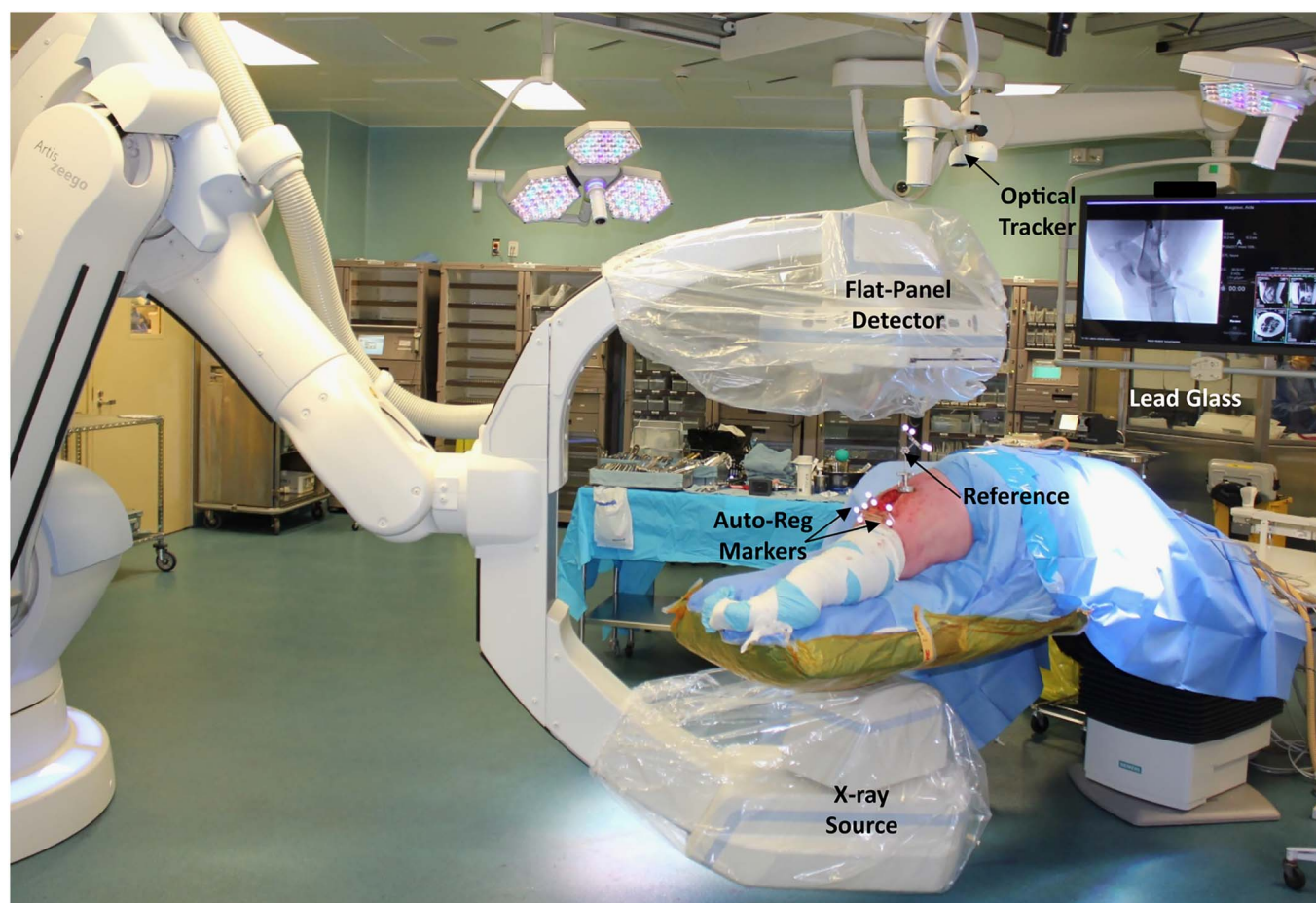


Fig. 1
Setup of the navigation system, with systems for robotic CBCT (Artis Zeego) and real-time optical tracking (Polaris Vicra; NDI). The UTs (automatic registration [auto-reg] markers) placed on the skin and the rigid reference (attached to the bone) can be seen positioned on the patient.

number; and (2) the target registration error (TRE), presented as a color-coded map over the bone surface. These registration metrics are well described in navigation literature^{28,29}. Briefly, the FRE measures the mean distance between fiducial points after registration. This is a commonly used metric that presents error as a single number (typically in millimeters); however, this only

pertains to fiducials. As the accuracy of rigid registration varies over the imaging volume, the more clinically relevant question is: what is the error associated with my current tool position? To quantify this, TRE measures the 3D distribution of navigation accuracy²⁹. Following guidelines to minimize the TRE (i.e., widely spaced fiducials with a centroid near the tumor)³⁰, the 2

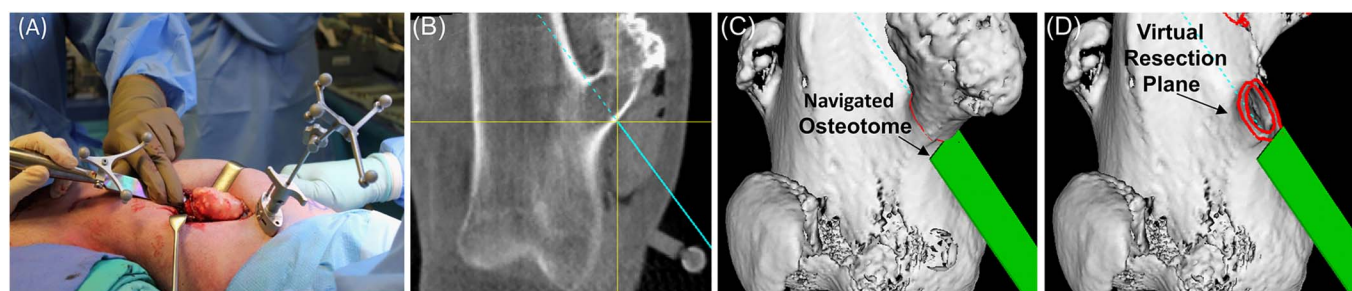


Fig. 2
Fig. 2-A An osteotome tracked by navigation was employed to resect the tumor guided by the in-house navigation software. **Figs. 2-B and 2-C** Visualization of the entire trajectory of the cutting instrument with respect to the tumor is shown in a 2D view (**Fig. 2-B**) and a 3D view (**Fig. 2-C**). **Fig. 2-D** The 3D view also has the ability to show a virtual resection using dynamic clipping planes.

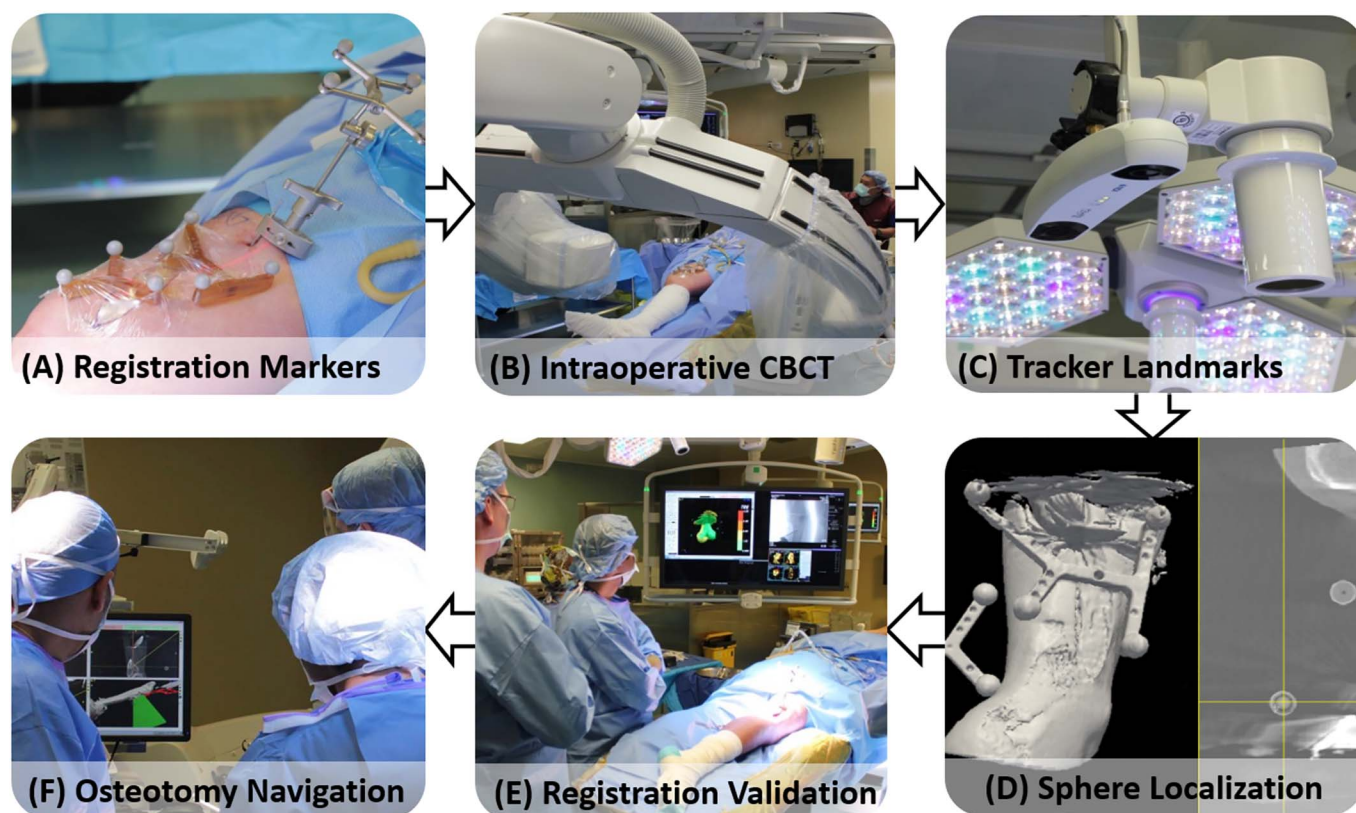


Fig. 3
Imaging and navigation workflow. **Fig. 3-A** Two UTTs with 3 and 4 spheres each secured to the skin overlying the bone lesion with sterile adhesive. The rigid tracker mounted to the bone adjacent to the tumor using cortical pins is also displayed. **Fig. 3-B** An intraoperative CBCT scan is obtained after rotation of the C-arm. **Fig. 3-C** The corresponding tracker landmarks were captured using an NDI Polaris infrared camera. **Fig. 3-D** The centers of the tracking spheres in CBCT imaging were localized automatically. **Fig. 3-E** The navigation system accuracy over the bone surface was depicted in a color-coded surface rendering. **Fig. 3-F** Surgical resection assisted by intraoperative navigation of cutting tools (e.g., osteotomes, saws) was performed using the in-house navigation software (GTx-Eyes, University Health Network).

surface-skin UTTs were positioned to meet 2 requirements: (1) placement as far apart from each other as possible while still being in the imaging volume, and (2) not lying in the same plane but instead wrapping around the tumor (Fig. 4-A). As an illustration in a representative case, we compared using 2 surface-skin UTTs wrapping around the surgical site for registration (Fig. 4-B) with 1 UTT (Fig. 4-C). Here, the TRE values are shown as color-coded bone surfaces. As theoretically predicted, the 2 UTTs provided the lowest TRE. We also utilized the traditional registration technique of choosing anatomical points in the initial 4 cases. This was achieved using intraoperative CBCT images, compared with using preoperative data as is typical for navigation systems. A total of 5 to 7 points along the exposed bone surface (Fig. 4-D) were manually localized in the CBCT scans and were registered using a tracked pointer.

Outcomes

The main outcomes were the FRE and TRE. These were computed within the in-house navigation software using previously defined equations³⁰. For each case, the FRE was a

single number, and the TRE was defined at each point on the bone surface. The FRE and TRE results are reported as the mean and the standard deviation, along with the range, over the patient cases. The bone surface was automatically generated using threshold surface rendering techniques in our navigation software²³. For each case, the mean and standard deviation of the TRE values over the bone surface were computed using MATLAB software (MathWorks). We also accounted for navigation time.

Source of Funding

This work was supported by the Strobele Family GTx Research Fund, Kevin and Sandra Sullivan Chair in Surgical Oncology, Hatch Engineering Fellowship Fund, RACH Fund, and Princess Margaret Hospital Foundation.

Results

The UTTs introduced minimal CT artifact. The mean values (and standard deviation) were 0.67 ± 0.15 mm (range, 0.47 to 0.97 mm) for the FRE and 0.83 ± 0.51 mm (range, 0.42 to 2.28 mm) for the TRE (Figs. 5-A and 5-B). The mean distance

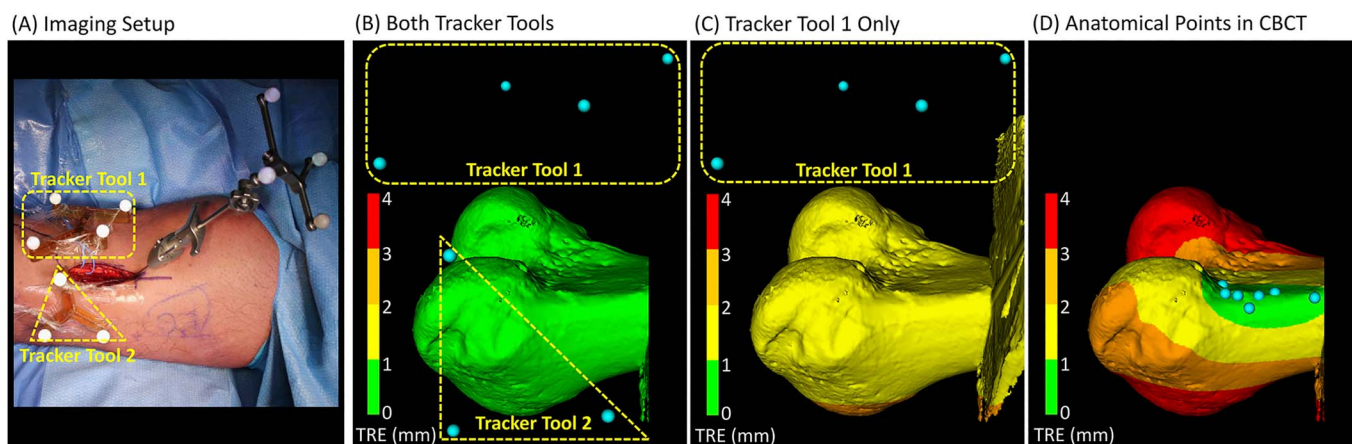


Fig. 4 Color-coded TRE maps using 3 registration techniques for the case of osteoid osteoma of the distal part of the right femur. The TRE in 4 distinct intervals was mapped to green (0 to 1 mm), yellow (>1 to 2 mm), orange (>2 to 3 mm), and red (>3 mm). **Fig. 4-A** Two UTTs were placed on the skin surface and the rigid tracking tool was attached to the exposed bone during CBCT scanning. **Fig. 4-B** Automatic registration using both skin UTTs that widely covered the surgical field. **Fig. 4-C** Automatic registration using only a single skin UTT for illustration. **Fig. 4-D** Manual, paired-point registration using anatomical landmarks visible on the exposed bone surface based on intraoperative CBCT imaging.

of separation between the UTTs was 9.9 ± 3.2 cm. The mean time required for CBCT imaging and registration was 7.5 minutes (range, 5 to 10 minutes). Registration was successful in all cases. Manual registration using bone surface points yielded TRE distributions that worsened with distance from the points (Fig. 4-D). Over the first 4 cases, the mean TRE was 2.54 ± 1.54 mm for manual registration and 0.76 ± 0.36 mm for automatic registration. Six of the pedunculated osteochondromas were resected using a single navigated osteotomy, and the removal of the other 3 pedunculated tumors and the 3 sessile lesions each required multiple navigated osteotomies. The osteoid osteoma was removed with a navigated burr. Pathology and post-resection imaging confirmed the complete resection of all lesions.

Discussion

We report a method of automatic registration using custom metal-free tools and intraoperative CBCT technology linked with a surgical navigation system²³⁻²⁵ and its results in a clinical cohort of 13 patients with benign bone tumors of the extremities. This registration technique provided highly accurate FRE (mean, 0.67 ± 0.15 mm) and TRE (mean, 0.83 ± 0.51 mm), with minimal additional operative time. Although these straightforward surgical cases did not require multiplanar navigated osteotomies, they served as simple, minimal-risk cases to validate accuracy in an initial pilot series.

Because CAS demonstrated enhanced precision in spine surgery and hip and knee arthroplasty^{31,32}, orthopaedic oncologists endeavored to exploit the benefits of this technology. The

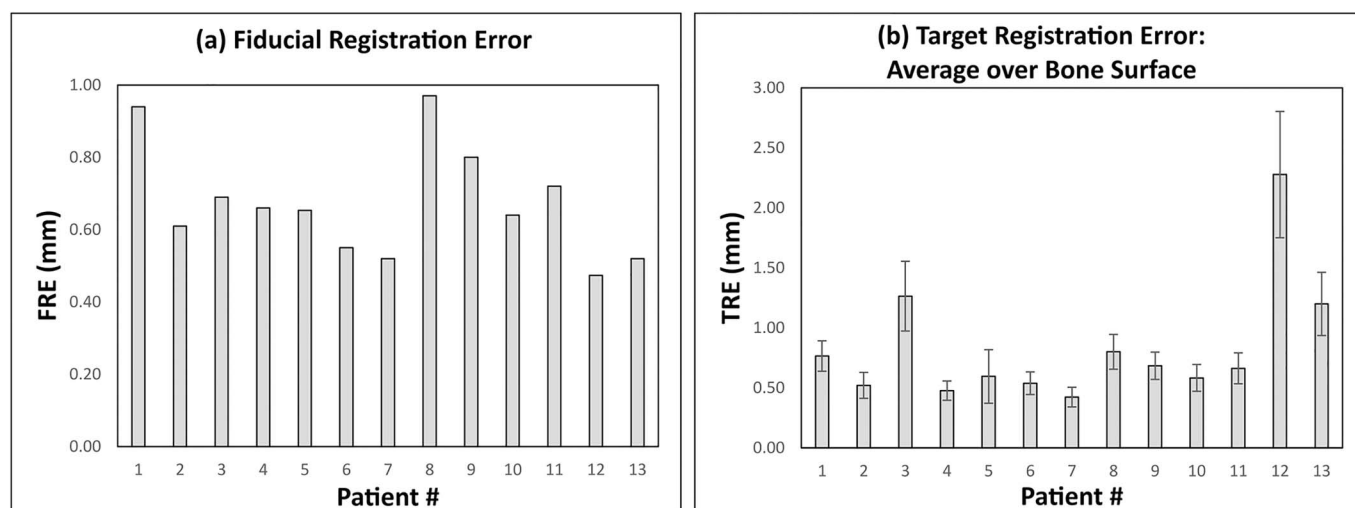


Fig. 5 **Fig. 5-A** The FRE for each case. **Fig. 5-B** The mean TRE computed over the bone surface. The error bars are ± 1 standard deviation.

potential for reduced surgical exposure and improved safety related to the proximity of vital, functional structures during pelvic bone tumor surgery make CAS especially appealing. Navigation has shown promising results, reducing intralesional resection rates for pelvic and sacral tumors⁹ and improving margins³³. Improved disease-free survival and reduction in blood loss and operative times were also reported³⁴. Joint-preserving resections for extremity bone sarcomas require high accuracy that can be facilitated with CAS¹⁰. Different 3D virtual resection scenarios can be analyzed preoperatively^{35,36}, followed by implementation of the best plan for complete tumor removal and reconstruction. CAS has improved tumor resection precision, allowing negative margins and preservation of articular surfaces. This provides enormous benefits for limb-sparing surgery, especially in skeletally immature patients¹¹. Different limb reconstruction alternatives using allografts and modular and custom-made prostheses are facilitated, and limb-length discrepancies and rotational concerns can be prevented^{12,24,37}.

Registration remains the most critical step in CAS, and discrepancies in registration can jeopardize resection accuracy. We developed an approach tailored to our intraoperative CBCT capabilities that enables accurate registration. We first placed a rigid tracker into the bone adjacent to the surgical field. Then we implemented the use of metal-free markers placed on the skin in the region of the tumor that act as surrogates, instead of using anatomic skeletal fiducial points. In a cadaveric study, Zamora et al.³⁸ found that both methods had comparable accuracy rates, but cutaneous fiducials represented a less invasive and more efficient method than extensive bone exposure to allow the identification of landmarks. Furthermore, by obtaining intraoperative imaging and using this automatic registration method, we eliminated the need for manual registration based on bone landmarks or surface tracing, which takes time, often requires more extensive surgical exposure than otherwise required for resection without navigation, and sometimes fails completely. Automatic registration added to the efficiency of CAS, as it only added a mean of 7.5 minutes. Previous studies using a combination of anatomic points and surface mapping for registration added means of 31 to 35 minutes^{12,21}. In some areas, skin fiducials may be more challenging to affix in an optimal configuration, which may explain the greater registration errors in Patient 12, who had a tumor located in the proximal part of the femur, and Patient 13, with a tumor located in the proximal part of the humerus. Our proposed approach for automatic registration is to scan and register prior to operative exposure (Fig. 3-A) or following only a limited exposure (Figs. 1 and 4-A). Therefore, skin adhesives were used, on the assumption that that imaging and registration would take place prior to a large operative exposure. One possible future extension to our approach would be to suspend the registration markers directly above the surgical field using a radiolucent support, which would allow for registration after large operative exposures.

A registration error of <1 to 2 mm has been deemed acceptable for CAS in bone sarcomas³⁹. We encountered a low FRE with a mean value of 0.67 mm. In a series of 66 patients who underwent limb-salvage surgery for bone tumors using a bone-inserted tracker and surface mapping, Aponte-Tinao et al.¹²

observed a mean registration error of 0.65 mm (range, 0.3 to 1.2 mm). We also reported the TRE, which is more clinically relevant, as it quantifies the error with respect to tool positioning. We observed a high degree of TRE accuracy, with a mean value of 0.83 ± 0.51 mm. The TRE captures errors beyond the fiducial points, which is a technical concept but crucial when high degrees of accuracy are needed to facilitate negative margins. Stoll et al. used bone-fixed light-emitting diodes as anatomical landmarks, followed by surface registration, and the results indicated a large registration error with substantial variability in accuracy and poor correlation with direct measurements obtained in bone tumor resections¹⁷. The mean measurement error, defined as the difference between post-registration points and planned registration points, was 12.21 ± 6.52 mm (range, 4.94 to 22.89 mm), and was significantly higher than the system-reported error of 0.68 ± 0.15 mm (range, 0.46 to 0.91 mm). This discrepancy advocates for more precision during registration¹⁷. In comparison, our autoregistration technique provided a low FRE and TRE.

With regard to UTT positioning, the first step is to ensure that the spheres lie completely within the CBCT volume. We followed guidelines to ensure that the spheres covered as wide an area as possible and had a centroid near the area of main interest³⁰. The best configuration strategy is depicted in Figure 4-A, with the UTTs lying at 90° to one another. Ideally, 2 UTTs should surround the area of interest and have a wide spacing, yielding a TRE of <1 mm over the majority of the bone surface (Fig. 4-B). The mean separation of our UTTs, at 9.9 cm, facilitated a minimal TRE. Ensuring that the UTT registration spheres lie completely within the CBCT volume (in this study, 25 × 25 × 18 cm) may be challenging in obese patients or those with large, deep tumors; however, 1 possible solution would be to automatically stitch together 2 acquisitions to encompass a larger volume⁴⁰. Using 1 UTT provided wide coverage but the spheres did not encircle the target, leading to a higher TRE of >1 mm (Fig. 4-C). As an alternative, we also used the common manual technique of identifying points on the exposed bone surface. However, this demonstrated a TRE of <1 mm only at points very close to the anatomical fiducials, with the error progressively increasing with distance (Fig. 4-D), illustrating the inaccuracy associated with this method in cases of limited bone exposure. Furthermore, the error associated with using anatomical fiducials in our study was likely underestimated by using intraoperative CBCT, compared with the more usual situation in which anatomical points identified on preoperative images are identified on the bone surface and linked together through the registration process.

Our main limitation was the lack of formal virtual margin assessment, which represents the ultimate confirmation of bone tumor surgery. Moreover, because patients with simple benign bone tumors were enrolled in this proof-of-principle study, the bone cuts were limited in size and extent compared with what would be required for malignant tumors. Nevertheless, all of the tumors were completely resected, and multiple navigated osteotomies were performed for 6 osteochondromas and a navigated burr was used to remove the osteoid osteoma. We acknowledge that surgical resection for osteoid osteoma is rarely necessary due to the high success rate


of RFA; however, this patient had undergone 2 unsuccessful CT-guided RFA attempts. It would have been interesting to confirm the previous findings of our group with regard to the accuracy of our navigation software, especially having intraoperative CBCT scans available, as we could have compared preoperative and postoperative resection plans to quantify the discrepancy due to not only registration error but also instrument calibration and user implementation^{24,25}.

First, we validated the registration accuracy in a small clinical cohort of patients with fairly simple benign tumors, for which there is no need for complex multiplanar navigated osteotomies, as part of a proof-of-principle study. We only performed manual registration in 4 cases to illustrate the TRE results compared with the automatic registration technique (Fig. 4). The TRE results would likely have been even worse if they had been based on preoperative imaging, rather than intraoperative CBCT as shown here and as documented in the study by Stoll et al.¹⁷. We compared our automatic registration results to a simple manual approach using only a few anatomical points, which could have been improved if surface matching was subsequently applied; future studies in pelvic surgery will compare our approach with surface-matching techniques in terms of both accuracy and ease of use. Our group is currently translating this system to treat more aggressive histologies and to navigate insertion of prostheses and allografts used for bone and joint reconstruction. Another limitation of our study involved its generalizability. Our registration method was designed for intraoperative CT capabilities, and not all centers have this resource. More widespread clinical adoption of in-room CT would require sufficient data on clinical benefits to justify equipment costs⁴¹. Some intraoperative CT systems provide automatic registration through the use of tracker markers affixed to the imaging device⁴²; further research is required to directly compare our method with these devices in terms of both registration accuracy and workflow efficiency. Alternatively, automatic registration techniques using optical technology, such as the Machine-vision Image Guided Surgery (MvIGS) system (7D Surgical), provide radiation-free scanning⁴³ but require bone exposure, which may be challenging in some settings (e.g., pelvic resection). Advantages associated with intraoperative CT imaging have recently been reported⁴⁴, and as this becomes more widely available, our automatic registration method could be employed to improve surgical efficiency. Our software was developed in-house, building on open-source software toolkits, and we surmise that this could also be applied in collaboration

with multidisciplinary translational navigation laboratories at other centers to enable more widespread clinical evaluation.

In conclusion, we present an automatic registration method for CAS for the resection of extremity bone tumors; this method showed improved results, including reduced operative times, compared with more traditional methods. The next step is to implement this approach for the treatment of patients with bone sarcomas, utilizing both preoperative and postoperative imaging and margin assessments to determine accuracy, as negative margins are critical to avoiding local tumor relapses, which have a profound negative impact on patient outcomes.

Appendix

 Supporting material provided by the authors is posted with the online version of this article as a data supplement at [jbjs.org \(http://links.lww.com/JBJSOA/A387\)](http://links.lww.com/JBJSOA/A387). ■

Axel Sahovaler, MD^{1,2}
 Michael J. Daly, PhD¹
 Harley H.L. Chan, PhD¹
 Prakash Nayak, MD^{1,3,4,5}
 Sharon Tzelnick, MD¹
 Michelle Arkhangorodsky, BSc¹
 Jimmy Qiu, MSc¹
 Robert Weersink, PhD¹
 Jonathan C. Irish, MD, MSc, FRCSC¹
 Peter Ferguson, MD, MSc, FRCSC^{1,4,5}
 Jay S. Wunder, MD, MSc, FRCSC^{1,4,5}

¹Guided Therapeutics (GTx) Program, TECHNA Institute, University Health Network, Toronto, Ontario, Canada

²Head & Neck Surgery Unit, University College London Hospitals, London, United Kingdom

³Department of Surgical Oncology, Bone and Soft Tissue Disease Management Group, Tata Memorial Centre, Mumbai, India

⁴Division of Orthopaedic Surgery, Department of Surgery, University of Toronto, Toronto, Ontario, Canada

⁵University of Toronto Musculoskeletal Oncology Unit, Mount Sinai Hospital, Toronto, Ontario, Canada

Email for corresponding author: jay.wunder@sinaihealth.ca

References

- Picci P, Sangiorgi L, Bahamonde L, Aluigi P, Bibiloni J, Zavatta M, Mercuri M, Briccoli A, Campanacci M. Risk factors for local recurrences after limb-salvage surgery for high-grade osteosarcoma of the extremities. *Ann Oncol*. 1997 Sep;8(9):899-903.
- Aponte-Tinao L, Ayerza MA, Muscolo DL, Farfalli GL. Survival, recurrence, and function after epiphyseal preservation and allograft reconstruction in osteosarcoma of the knee. *Clin Orthop Relat Res*. 2015 May;473(5):1789-96.
- Bus MP, Brammer JA, Schaap GR, Schreuder HW, Jutte PC, van der Geest IC, van de Sande MA, Dijkstra PD. Hemicortical resection and inlay allograft reconstruction for primary bone tumors: a retrospective evaluation in the Netherlands and review of the literature. *J Bone Joint Surg Am*. 2015 May 6;97(9):738-50.
- Lewis VO, Gebhardt MC, Springfield DS. Parosteal osteosarcoma of the posterior aspect of the distal part of the femur. Oncological and functional results following a new resection technique. *J Bone Joint Surg Am*. 2000 Aug;82(8):1083-8.
- Sternheim A, Rotman D, Nayak P, Arkhangorodsky M, Daly MJ, Irish JC, Ferguson PC, Wunder JS. Computer-assisted surgical planning of complex bone tumor resections improves negative margin outcomes in a sawbones model. *Int J Comput Assist Radiol Surg*. 2021 Apr;16(4):695-701.

6. Muscolo DL, Ayerza MA, Aponte-Tinao LA, Ranalletta M. Partial epiphyseal preservation and intercalary allograft reconstruction in high-grade metaphyseal osteosarcoma of the knee. *J Bone Joint Surg Am*. 2005 Sep;87(Pt 2)(Suppl 1):226-36.
7. Deijkers RLM, Bloem RM, Kroon HM, Van Lent JB, Brand R, Taminiau AHM. Epidiaphyseal versus other intercalary allografts for tumors of the lower limb. *Clin Orthop Relat Res*. 2005 Oct;439:151-60.
8. Cho HS, Oh JH, Han I, Kim HS. The outcomes of navigation-assisted bone tumor surgery: minimum 3-year follow-up. *J Bone Joint Surg Br*. 2012 Oct;94(10):1414-20.
9. Jeys L, Matharu GS, Nandra RS, Grimer RJ. Can computer navigation-assisted surgery reduce the risk of an intralesional margin and reduce the rate of local recurrence in patients with a tumour of the pelvis or sacrum? *Bone Joint J*. 2013 Oct;95-B(10):1417-24.
10. Wong KC, Kumta SM. Joint-preserving tumor resection and reconstruction using image-guided computer navigation. *Clin Orthop Relat Res*. 2013 Mar;471(3):762-73.
11. Li J, Shi L, Chen GJ. Image navigation assisted joint-saving surgery for treatment of bone sarcoma around knee in skeletally immature patients. *Surg Oncol*. 2014 Sep;23(3):132-9.
12. Aponte-Tinao L, Ritacco LE, Ayerza MA, Muscolo DL, Albergo JI, Farfalli GL. Does intraoperative navigation assistance improve bone tumor resection and allograft reconstruction results? *Clin Orthop Relat Res*. 2015 Mar;473(3):796-804.
13. Muhanna N, Douglas CM, Daly MJ, Chan HHL, Weersink R, Qiu J, Townson J, de Almeida JR, Goldstein D, Gilbert R, Yu E, Kucharczyk W, Jaffray DA, Irish JC. The image-guided operating room-utility and impact on surgeon's performance in the head and neck surgery. *Head Neck*. 2019 Sep;41(9):3372-82.
14. Liu WP, Otake Y, Azizian M, Wagner OJ, Sorger JM, Armand M, Taylor RH. 2D-3D radiograph to cone-beam computed tomography (CBCT) registration for C-arm image-guided robotic surgery. *Int J Comput Assist Radiol Surg*. 2015 Aug;10(8):1239-52.
15. Dea N, Fisher CG, Batke J, Strelzow J, Mendelsohn D, Paquette SJ, Kwon BK, Boyd MD, Dvorak MF, Street JT. Economic evaluation comparing intraoperative cone beam CT-based navigation and conventional fluoroscopy for the placement of spinal pedicle screws: a patient-level data cost-effectiveness analysis. *Spine J*. 2016 Jan 1;16(1):23-31.
16. Schep NWL, Broeders IAMJ, van der Werken C. Computer assisted orthopaedic and trauma surgery. State of the art and future perspectives. *Injury*. 2003 May;34(4):299-306.
17. Stoll KE, Miles JD, White JK, Punt SEW, Conrad EU 3rd, Ching RP. Assessment of registration accuracy during computer-aided oncologic limb-salvage surgery. *Int J Comput Assist Radiol Surg*. 2015 Sep;10(9):1469-75.
18. Wong KC, Kumta SM, Chiu KH, Antonio GE, Unwin P, Leung KS. Precision tumour resection and reconstruction using image-guided computer navigation. *J Bone Joint Surg Br*. 2007 Jul;89(7):943-7.
19. Docquier PL, Paul L, Cartiaux O, Delloye C, Banse X. Computer-assisted resection and reconstruction of pelvic tumor sarcoma. *Sarcoma*. 2010;2010:125162.
20. Ritacco LE, Milano FE, Farfalli GL, Ayerza MA, Muscolo DL, Aponte-Tinao LA. Accuracy of 3-D planning and navigation in bone tumor resection. *Orthopedics*. 2013 Jul;36(7):e942-50.
21. Farfalli GL, Albergo JI, Ritacco LE, Ayerza MA, Milano FE, Aponte-Tinao LA. What is the expected learning curve in computer-assisted navigation for bone tumor resection? *Clin Orthop Relat Res*. 2017 Mar;475(3):668-75.
22. Muhanna N, Douglas CM, Daly MJ, Chan HHL, Weersink R, Townson J, Monteiro E, Yu E, Weimer E, Kucharczyk W, Jaffray DA, Irish JC, de Almeida JR. Evaluating an image-guided operating room with cone beam CT for skull base surgery. *J Neurol Surg B Skull Base*. 2021 Jul;82(Suppl 3):e306-14.
23. Daly MJ, Chan H, Nithiananthan S, et al. Clinical implementation of intraoperative cone-beam CT in head and neck surgery. In: Wong KH, Holmes III DR, editors. *Proceedings of SPIE Medical Imaging*, 2011 Feb 13-15. Society of Photo-Optical Instrumentation Engineers; 2011.
24. Sternheim A, Daly M, Qiu J, Weersink R, Chan H, Jaffray D, Irish JC, Ferguson PC, Wunder JS. Navigated pelvic osteotomy and tumor resection: a study assessing the accuracy and reproducibility of resection planes in Sawbones and cadavers. *J Bone Joint Surg Am*. 2015 Jan 7;97(1):40-6.
25. Sternheim A, Kashigar A, Daly M, Chan H, Qiu J, Weersink R, Jaffray D, Irish JC, Ferguson PC, Wunder JS. Cone-beam computed tomography-guided navigation in complex osteotomies improves accuracy at all competence levels: a study assessing accuracy and reproducibility of joint-sparing bone cuts. *J Bone Joint Surg Am*. 2018 May 16;100(10):e67.
26. Bernstein JM, Daly MJ, Chan H, Qiu J, Goldstein D, Muhanna N, de Almeida JR, Irish JC. Accuracy and reproducibility of virtual cutting guides and 3D-navigation for osteotomies of the mandible and maxilla. *PLoS One*. 2017 Mar 1;12(3):e0173111.
27. Hasan W, Daly MJ, Chan HHL, Qiu J, Irish JC. Intraoperative cone-beam CT-guided osteotomy navigation in mandible and maxilla surgery. *Laryngoscope*. 2020 May;130(5):1166-72.
28. Fitzpatrick JM, West JB, Maurer CR Jr. Predicting error in rigid-body point-based registration. *IEEE Trans Med Imaging*. 1998 Oct;17(5):694-702.
29. Fitzpatrick JM, West JB. The distribution of target registration error in rigid-body point-based registration. *IEEE Trans Med Imaging*. 2001 Sep;20(9):917-27.
30. West JB, Fitzpatrick JM, Toms SA, Maurer CR Jr, Maciunas RJ. Fiducial point placement and the accuracy of point-based, rigid body registration. *Neurosurgery*. 2001 Apr;48(4):810-6, discussion 816-7.
31. Flynn JM, Sakai DS. Improving safety in spinal deformity surgery: advances in navigation and neurologic monitoring. *Eur Spine J*. 2013 Mar;22(S2)(Suppl 2):S131-7.
32. de Steiger RN, Liu YL, Graves SE. Computer navigation for total knee arthroplasty reduces revision rate for patients less than 65 years of age. *J Bone Joint Surg Am*. 2015 Apr 15;97(8):635-42.
33. Bosma SE, Cleven AHG, Dijkstra PDS. Can navigation improve the ability to achieve tumor-free margins in pelvic and sacral primary bone sarcoma resections? A historically controlled study. *Clin Orthop Relat Res*. 2019 Jul;477(7):1548-59.
34. Laitinen MK, Parry MC, Albergo JI, Grimer RJ, Jeys LM. Is computer navigation when used in the surgery of iliosacral pelvic bone tumours safer for the patient? *Bone Joint J*. 2017 Feb;99-B(2):261-6.
35. So TYC, Lam YL, Mak KL. Computer-assisted navigation in bone tumor surgery: seamless workflow model and evolution of technique. *Clin Orthop Relat Res*. 2010 Nov;468(11):2985-91.
36. Wong KC, Kumta SM. Computer-assisted tumor surgery in malignant bone tumors. *Clin Orthop Relat Res*. 2013 Mar;471(3):750-61.
37. Li J, Wang Z, Guo Z, Chen GJ, Yang M, Pei GX. Precise resection and biological reconstruction under navigation guidance for young patients with juxta-articular bone sarcoma in lower extremity: preliminary report. *J Pediatr Orthop*. 2014 Jan;34(1):101-8.
38. Zamora R, Punt SE, Christman-Skieller C, Yildirim C, Shapton JC, Conrad EU 3rd. Are skin fiducials comparable to bone fiducials for registration when planning navigation-assisted musculoskeletal tumor resections in a cadaveric simulated tumor model? *Clin Orthop Relat Res*. 2019 Dec;477(12):2692-701.
39. Wong KC, Kumta SM. Use of computer navigation in orthopedic oncology. *Curr Surg Rep*. 2014 Feb 22;2:47.
40. Fotouhi J, Fuerst B, Unberath M, Reichenstein S, Lee SC, Johnson AA, Osgood GM, Armand M, Navab N. Automatic intraoperative stitching of nonoverlapping cone-beam CT acquisitions. *Med Phys*. 2018 Jun;45(6):2463-75.
41. Tonetti J, Boudissa M, Kerschbaumer G, Seurat O. Role of 3D intraoperative imaging in orthopedic and trauma surgery. *Orthop Traumatol Surg Res*. 2020 Feb;106(1S):S19-25.
42. Sommer F, Goldberg JL, McGrath L Jr, Kimaz S, Medary B, Härtl R. Image guidance in spinal surgery: a critical appraisal and future directions. *Int J Spine Surg*. 2021 Oct;15(s2):S74-86.
43. Doriljo J, Utah N, Dowe C, Avrumova F, Alicea D, Brecevic A, Callanan T, Sama A, Lebl DR, Abjornson C, Cammisia FP. Comparing the efficacy of radiation free machine-vision image-guided surgery with traditional 2-dimensional fluoroscopy: a randomized, single-center study. *HSS J*. 2021 Oct;17(3):274-80.
44. Luxenhofer M, Beisemann N, Schnetzke M, Vetter SY, Grützner PA, Franke J, Keil H. Diagnostic accuracy of intraoperative CT-imaging in complex articular fractures - a cadaveric study. *Sci Rep*. 2020 Mar 11;10(1):4530.